INVESTIGATION OF THE TRANSIENT BEHAVIOUR OF A GRID-CONNECTED PHOTOVOLTAIC GENERATOR

[1]Michael O. OMOIGUI [2]Titus O. AJEWOLE and [3]Funso K. ARIYO

1, 3 Department of Electronic and Electrical Engineering
Obafemi Awolowo University
Ile-Ife, Nigeria.
E-mail: mikeomoigui@yahoo.co.uk
ariyofunso@yahoo.com

2 Department of Electrical and Electronic Engineering
Osun State University
Osogbo, Nigeria.
E-mail: toajewole2002@yahoo.com

Abstract

Installation of off-grid (stand-alone) photovoltaic (PV) generators as alternative electricity sources has been on the increase in developing countries. In Nigeria, the recent Federal Government policy of deregulating the electrical utility has brought the grid-connected PV technology into a great attention. However, possible transient consequences of using the technology are threats to its immediate adoption. This paper therefore presents a study on the transient behaviour of grid-connected photovoltaic generator. By experimenting with a simulated model of a typical grid-connected photovoltaic power system, the generator's response to faults applied at its terminals was investigated. The resulting waveforms reveal damped oscillatory behaviour of the terminal variables due to a symmetrical short circuit. Applications of non-symmetrical short-circuit also resulted to instability at the generator's terminals. Nevertheless, following the clearance of each fault, the system resumes its normal operation with the variables smoothly settled at their initial stable values. The investigation reveals that by providing protective devices and standard means of fault isolation, the possible effect of the instability on the entire system can be minimized.

KEYWORDS: *Photovoltaic generator, voltage source inverter, grid-connected, LC filter, fault, damped oscillation.*

Nomenclature

I_L	Photo-generated current of a solar cell.
I_o	Cell reverse saturation current.
exp	Exponential function.
e	Electronic charge.
n	Solar cell's empirical ideality factor.
k	Boltzmann's constant.
K	Temperature coefficient of a solar cell.
T_c	Solar cell's working temperature.
I_{scr}	Reference short-circuit current.
K	Temperature coefficient.
T_r	Reference temperature.
G_r	Reference solar intensity.
I_{or}	Reverse saturation current at reference.
E_g	Bang-gap energy of the semiconductor.
I, V	Solar cell's output current, voltage.
π	Phase shift in radians.
α, β	Numbers of parallel, series cells per array.
I_{pv}, V_{pv}	Current, voltage output of the array.
V_{dc}	Inverter's input bus voltage.
v_{ac}	Inverter's output terminal voltage.

L_f, C_f Inductance and capacitance of the filter.
R_f Parasitic resistance of the filter
v_c Voltage output of the filter.
i_d, i_q Direct, quadrature controller input current.
i_{d_r}, i_{q_r} Direct, quadrature reference current.
e_d, e_q Direct, quadrature the error current.
v_{c_d}, v_{c_q} Direct, quadrature filtered voltage.
$G_d(s), G_q(s)$ Direct, quadrature transfer functions.
m_d, m_q Direct, quadrature Output signals.
m_1, m_2, m_3 Modulating signals.

INTRODUCTION

Photovoltaic (PV) conversion of solar radiant energy is gaining higher acceptance compared to other resources mankind has harnessed to generate electricity. Despite the relatively high cost and low efficiency of the technology, it is significantly penetrating into the global energy mainstream by the reason of the abundance, accessibility and environmental friendliness of solar radiation. With the increasing demand for electrical energy in Nigeria, the new trend is Distributed Generation (DG) with intense focus on renewable sources. This has resulted into a progressive tendency in the application of solar energy technology across the country, since PV power can be extended for residential, commercial, and agricultural uses to mention a few.

The electrical resource of the sun is explored using either off-grid (stand-alone) or grid-connected PV techniques. Off-grid PV generators are either used as stand-by alternative power sources or employed in some other cases to produce all the power requirements of a facility, thus making the user of the technology to be completely independent from the utility company.

This paper is however concerned with the grid-connected PV power system, which is a mode of power generation that is possible in either non-commercial or commercial sizes. Non-commercial one is the small, single-phase generation usually installed at the consumer end which allows the use of PV generator to supply most of the base load of the facility while using the utility company only within the short peak load hours. Excess PV power generated during the peak solar window can be fed back to the local utility provided net-metering technique is put in place.

Nonetheless, when PV power is to be generated in commercial size, the supply is usually in three-phase. This therefore prompts the integration of the PV generator with the conventional utility grid at either the sub-transmission or the distribution level, for a convenient distribution of the energy so generated.

The grid-connected mode of PV technology has not achieved prominence in Nigeria for technical and economic reasons. Interfacing a PV generating plant with the utility grid poses some transient consequences that must be taken into account or resolved to ensure a good quality of operation. Thus in the view of the increasing need for multi-megawatt PV generation, and in response to the utility company's concerns about the possible negative impacts of grid-tied PV power systems on both feeders and customers, the increasing pace of investigations on PV system's dynamics properties and transient performances is of great importance.

A large number of works have been done on photovoltaic power system, which includes system's modeling, maximum power point tracking techniques and transient study. Tsai et al. (2008) described various types of equivalent circuit-based mathematical description of solar cell (and array) useful for modeling a PV system for transient studies. The maximum power point tracking of PV systems has been widely studied. Nikraz et al. (2003) proposed a DSP-based tracking mechanism. In the work, tracking control is provided by a 16-bit fixed-point TI TMS320F240 DSP processor that provides automatic adjustment of the array's reference voltage, resulting in an improved overall effectiveness. More recently, Patcharaprakiti et al. (2008) adopted a tracking approach that uses Adaptive Fuzzy Logic Controller (AFLC), which provides more energy to the utility grid at high power factor and with low harmonics.

Integration of PV systems with distribution networks have been dealt with in certain technical literatures. The works of Abo-Khalil et al. (2007) described the modeling of single-phase grid-connected PV system to study its harmonic interactions with the distribution network. Yazdani and Dash (2008) reviewed eleven different works on this aspect and elegantly developed a mathematical model for the performance evaluation of a single-stage three-phase grid-connected PV system with provision for islanding detection and protection. Ajewole (2010) emphasized fault analysis on a grid-integrated PV power system and surveyed the response of a simulated PV system to faults applied at an arbitrarily selected point on the system.

In this paper however, the transient response of a grid-connected PV generator to short circuits that occurs at the generator's terminals is reported. The study was carried out by simulating a model of a typical grid-connected PV system on the MATLAB/Simulink power system simulation software. Current control of the system was adopted for the simple circuitry and less mathematical complexity of the method. The system was then subjected to faults experimented at the terminals of the PV generator. The voltage/current profile of the generator's response is given and analyzed in this report.

I. SYSTEM CONFIGURATION AND MODELING

Figure 1 was configured on the platform of the simulation software. It is a three-phase single-stage PV-source embedded generation, connected to the grid through a 415V/11kV interface transformer. The array is a number of PV cells connected in series-parallel configuration and subjected to the same operating condition. Output of the array is connected to the voltage source inverter (VSI) through the link capacitor which stabilizes the voltage. A relatively smooth DC voltage at the input of the VSI allows good regulation which results in a system that works well with high accuracy.

The VSI is a universal type, employed to operate in the voltage-source mode, with IGBT/diodes as the switching devices. In order to prevent the spurious voltage output of the VSI's high-frequency switching noises from disturbing the distribution network, a low-pass LC filter is included, whose output is serially connected to the primary side of an interface transformer. The transformer serves as the coupler between the PV facilities and the grid, so providing galvanic separation of the facilities from the electric utility at the point of common coupling. Finally, to serve as a means of isolating the inverter from the grid during servicing or installation, a circuit breaker is included.

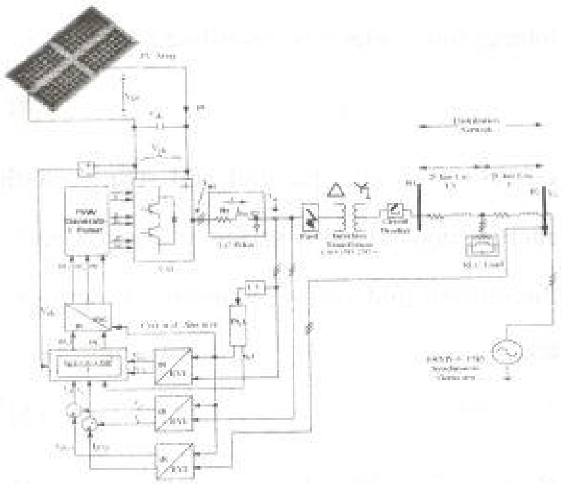

Figure 1: Structure of a Grid-Connected Photovoltaic Power System

II.I. Modeling of the PV Array

With the standard operating condition (1000W/m^2 and 300 Kelvin) taken as the reference, the PV cells are assumed as ideal ones, in which there is neither series loss nor leakage to the ground. That is, the series resistance $R_s = 0$ and the parallel resistance $R_p = \infty$ for each of the cells. Therefore, the output current and voltage per singular cell are:

$$I = I_L - I_o[exp(\frac{eV}{nkT_c}) - 1]; \quad (1)$$

$$V = \frac{nkT_c}{e} ln\left[\frac{I_L - I + I_o}{I_o}\right] \quad (2)$$

The photo-generated current, which mainly depends on the solar radiation intensity and the cell's working temperature, is described as:

$$I_L = [I_{scr} + K(T_c - T_r)]G_r \quad (3)$$

I_{scr} is determined from the cell's conversion efficiency, which is the ratio of the maximum output power to the input power of the cell. Likewise, the cell's reverse saturation current varies with the cell temperature, which is described as:

$$I_o = I_{or}\left[\frac{T_c}{T_r}\right]^3 exp\left[\frac{eE_g}{nk}\left(\frac{1}{T_r}-\frac{1}{T_c}\right)\right] \quad (4)$$

For an array of α parallel cell strings, with each string having β series-connected cells, the current and voltage outputs of the array are:

$$I_{pv} = \alpha I_L - \alpha I_0\,[exp(\frac{eV_{pv}}{\beta nkT}) - 1] \quad (5)$$

$$V_{pv} = \beta(\frac{nkT}{e} ln\left[\frac{I_L - I + I_0}{I_0}\right]) \quad (6)$$

Equations (6) was coded in the MATLAB Editor and exported to the simulink environment to simulate the PV array.

II.II. Modeling of the VSI

With the assumption that the inverter is of high efficiency with negligible loss, it is modeled with its input/output inversion ratio. The input DC voltage, V_{dc}, of the inverter and its peak phase-to-phase output voltage, v_{ac}, are related by:

$$v_{ac} = \frac{m\sqrt{2}}{2} V_{dc} \quad (7)$$

where m, is the modulation ratio commonly used for the conventional VSI. R_f is the parasitic-resistance of the LC-filter, which is included to account for inductor and capacitor losses. The peak phase-to-phase voltage output of the inverter is therefore described by:

$$v_{ac} = \sqrt{2}[R_f i + L_f \frac{di}{dt} + v_c] \quad (8)$$

Where v_c is the voltage output of the filter as obtained across the terminals of the filter's capacitor. By substituting equation (7) into (8) we obtain;

$$m = \frac{2}{v_{dc}}[R_f i + L_f \frac{di}{dt} + v_c] \quad (9)$$

Equation (9) describes the dynamic behavior of the PV generator's output, so employed for the system's control. However, by converting the time-dependent variables of the equation into their DC equivalents, the control process can be made more convenient. Three-phase variables, with the exception of their zero-sequence components can be equivalently represented by two-dimensional complex space vector when transformed on a stationary d-q reference frame as described below (Ryu et al., 2005):

$$y^r_{dq} \equiv y^s_{dq}\, e^{j\theta} = (\, y^s_d + j y^s_q\,) e^{j\theta} \quad (10)$$

where ($\theta = \int \omega dt$) is the rotating angle of the frame and ω denotes the fundamental frequency or the angular velocity of the reference field. y^s_d and y^s_q are the respective direct and quadrature components of the reference frame vector y^r_{dq}. Taking the time-varying variables to have the sinusoidal frequency ω_g of the grid, while the fundamental rotating frequency of the reference field is taken as ω_r, then at steady state, the d-q components of the frame become time-invariant (i.e. dc equivalent) if ω_r is made equal to ω_g. Therefore, when m in equation (9) is projected on the reference frame it becomes m_{dq}:

$$m_{dq} = (m_d + jm_q)e^{j\theta} \quad (11)$$

$$m_{dq} = \frac{2}{v_{dc}}\left[R_f(i_d + ji_q) + L_f\left\{\frac{d(i_d + ji_q)}{dt}\right\} + (v_{c_d} + jv_{c_q})\right]e^{j\theta} \quad (12)$$

$$m_{dq} = \frac{2}{v_{dc}}\left[R_f(i_d + ji_q) + L_f\left\{\left(\frac{di_d}{dt} + j\frac{di_q}{dt}\right) + j\omega_r(i_d + ji_q)\right\} + (v_{c_d} + jv_{c_q})\right]e^{j\theta} \quad (13)$$

Separating the real and the imaginary parts of equation (13), we obtain for the direct-axis and the quadrature-axis respectively as;

$$m_d = \frac{2}{V_{dc}}\left[R_f i_d + L_f\frac{di_d}{dt} - \omega_r L_f i_q + v_{c_d}\right] \quad (14)$$

and;

$$m_q = \frac{2}{V_{dc}}\left[R_f i_q + L_f\frac{di_q}{dt} + \omega_r L_f i_d + v_{c_q}\right] \quad (15)$$

At each of the axis, the control inputs is i_d and i_q, while the control output is m_d and m_q respectively. To operate the process as a linear plant, the non-linearity introduced by the ω_r is decoupled and compensated for using controllers. A conventional proportional-integral-derivative (PID) controller is employed for each axis. It gives good transient as well as steady state control. However, the input to a controller is basically an error signal between the actual and a reference signal, so reference currents i_{d_r} and i_{q_r} were introduced to track i_d and i_q respectively. This results into error signals e_d and e_q, as inputs to the respective controller of each axis.

Since the controllers are identical, they were made to have the same parameters, with the following transfer function:

$$G_d(s) = \frac{K_p S + K_i + K_d S^2}{S} \quad (16)$$

and;

$$G_q(s) = \frac{K_p S + K_i + K_d S^2}{S} \quad (17)$$

K_p, K_i and K_d are proportional, integral and derivative gains respectively and their values are taken as $K_p = \frac{R_f}{\tau}$; $K_i = \frac{L_f}{\tau}$ and $K_d = \frac{C_f}{\tau}$; where τ is the time constant.

The index for the control scheme is therefore described for each axis as:

$$m_d = [\{e_d \times G_d(s)\} - \omega_r L_f i_q + v_{c_d}] \quad (18)$$

and;

$$m_q = \left[\{e_q \times G_q(s)\} + \omega_r L_f i_d + v_{c_q}\right] \quad (19)$$

With f_s as the switching frequency measured in hertz, the selection of the filter's inductance L_f, depends on the current ripple $i_{cr(p-p)}$, the switching frequency, the DC-bus voltage, and is obtained as (Singh et al., 2008):

$$L_f = \frac{m_a\sqrt{3}}{12 a f_s i_{cr(p-p)}} V_{dc} \quad (20)$$

In this study, $i_{cr(p-p)}$ is taken to be 5% as provided by the islanding control standards (IEEE 929-2000), while a is the overload factor.

Conditioning a six-pulse type of VSI requires three reference signals to be compared with the carrier signal of the PWM generator. Therefore, m_d and m_q were inverse-transformed into three signals using *dq-to-abc* transformation frame as given below:

$$m_1 = [m_d \sin(\omega_r t) + m_q cos(\omega_r t) + m_0]$$

$$m_2 = [m_d \, sin(\omega_r t - \tfrac{2\pi}{3}) + m_q cos(\omega_r t - \tfrac{2\pi}{3}) + m_0]$$

$$m_3 = [m_d \, sin(\omega_r t + \tfrac{2\pi}{3}) + m_q cos(\omega_r t + \tfrac{2\pi}{3}) + m_0] \quad (21)$$

m_1, m_2 and m_3 are the modulating signals that are compared with the triangular carrier signal of the pulse-width generator to produce the pulses that drive the gates of the six switching devices of the inverter. The continuous pulse width modulation (PWM) usually generates lower ripples compared to other designs of high-density modulator.

II. SIMULATION AND DISCUSSION OF RESULTS

The MATLAB coded script simulates the PV array with substituted parameter values of the GaAs/AlGaAs solar cell. Solar irradiation level and working temperature were held constant at 0.9 kW/m^2 and 315 Kelvin respectively. Each simulation experiment lasted for a period of 200 milliseconds with fault applied at the terminal of the generator at time $t = {}^4/_{60}$ seconds and cleared at time $t = {}^8/_{60}$ seconds. Figure 2 (a) and (b) shows the waveform of the terminal variables of the generator under normal start-up. The generator is regulated to produce an output voltage of 590 Vpeak (415 Vrms) and current is 95 ampere that feeds the primary side of the transformer.

As shown in figure 2 (c) and (d), the terminal variables are set into damped oscillation with the application of a symmetrical short circuit. The oscillatory nature is noticeable as voltage and current in the three phases decay gradually to steady-states. A physical explanation for this phenomenon is that prior to the short-circuit, energy was initially stored by the reactive components of the LC filter, which was continually dissipated to the grid via the interface transformer. When short-circuited, the energy is no more provided with a means of dissipation, so became continuously transferred back and forth between the capacitor C_f and the inductor L_f of the filter. The motion is however not perpetual, but short-lived with the presence of the finite-valued parasitic resistance R_f of the filter, which acts as a kind of electrical transfer agent. As the energy starts moving from C_f to L_f and vice versa, the agent exacts a commission and before long the agent has taken all the energy, wantonly dissipating it until every last joule is (eventually) completely damped-out, such that C_f and L_f are soon left without a joule of their own, and without voltage or current. The final steady-state level is maintained until the short-circuit is cleared.

The response of the generator to a single line-to-ground short-circuit on the red phase is shown in figure 2 (e) and (f). The terminal variables become unstable and both current and voltage on the short-circuited phase fall below their pre-fault values.

On the application of a line-to-line short-circuit between the red and the yellow phases; the generator's response is as shown in figure 2(g) and (h). While the voltage waveform shows a drop by 57% of the pre-fault value on both phases, the current waveform shows the red phase fall to zero level with a reduction from 105A to 85A on the other two phases.

In the case of a double line-to-ground short-circuit, the red and the yellow phases are connected to the ground. The response is demonstrated in figure 2(i) and (j) which show the voltage drop by 57% of the pre-fault value on the two phases and a drop of 19% on the third phase. The current waveform shows the red phase fall to zero level, while a reduction from 105A to 85A occurred on the other phases.

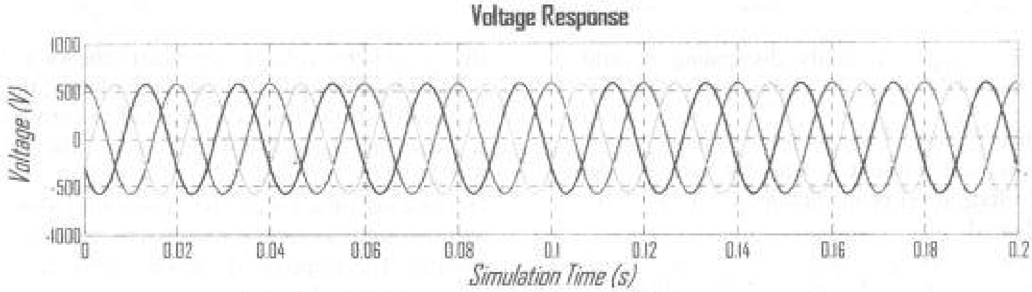

(a) Terminal Voltage under Normal Starting Operation.

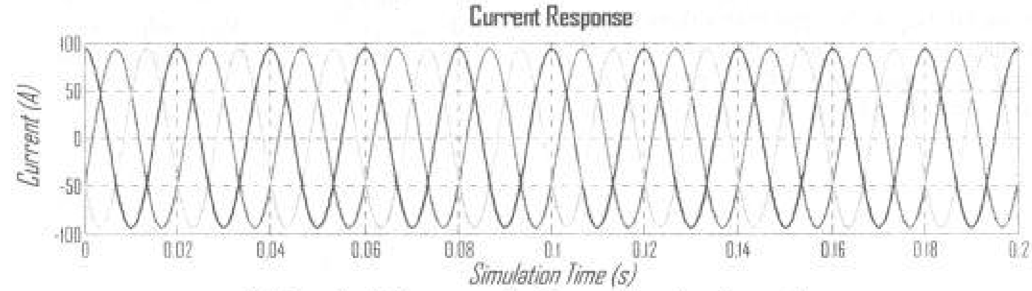

(b) Terminal Current under Normal Starting Operation.

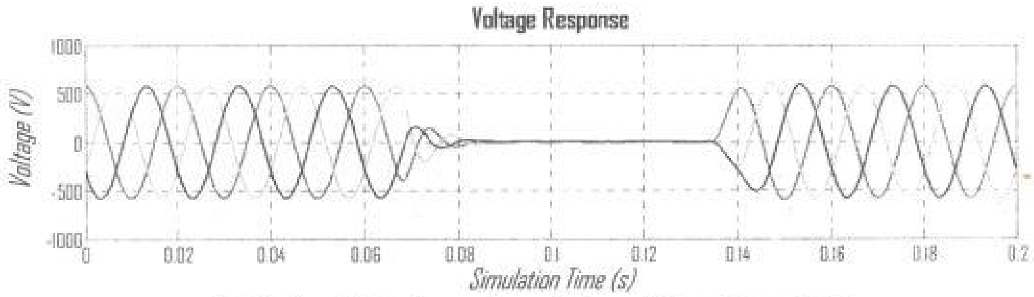

(c) Voltage Behaviour under a Balanced Three Phase Fault.

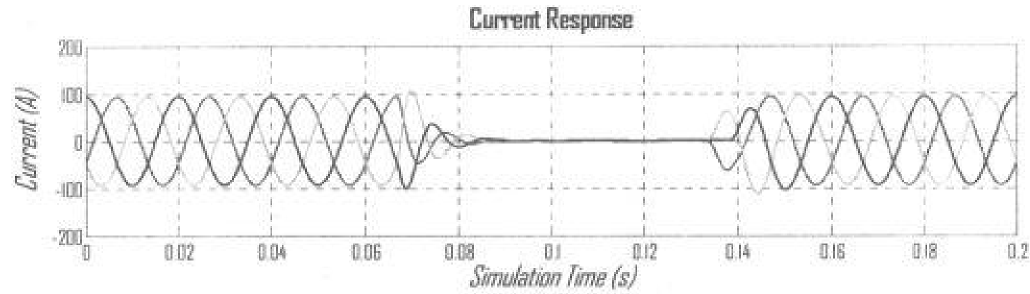

(d) Current Behaviour under a Balanced Three Phase Fault.

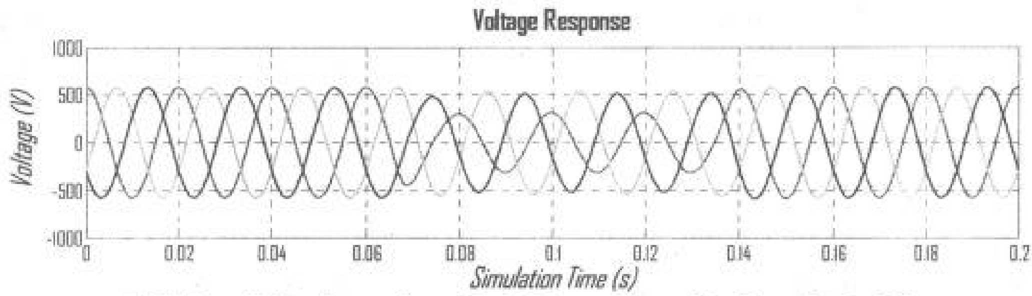

(e) Voltage Behaviour under a Single Line-to-Ground Fault on the Red Phase.

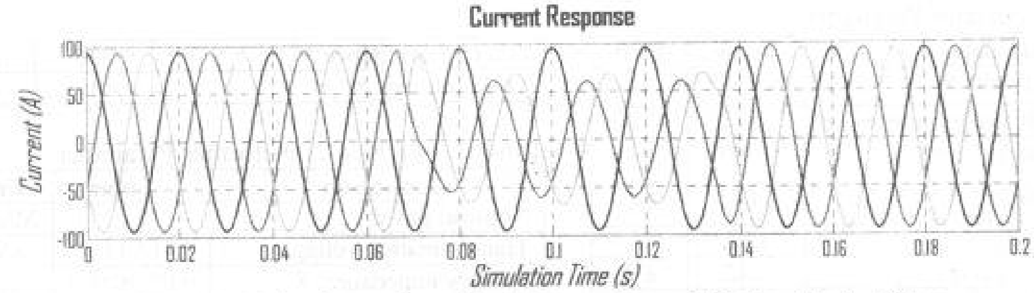

(f) Current Behaviour under a Single Line-to-Ground Fault on the Red Phase.

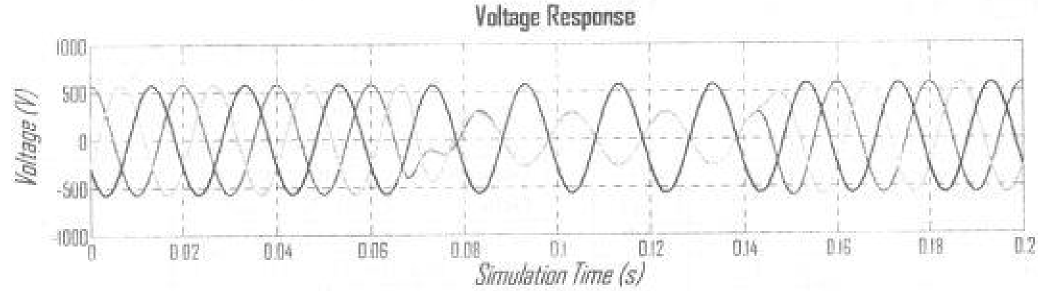

(g) Voltage Behaviour under a Line-to-Line Fault between the Red and the Yellow Phases.

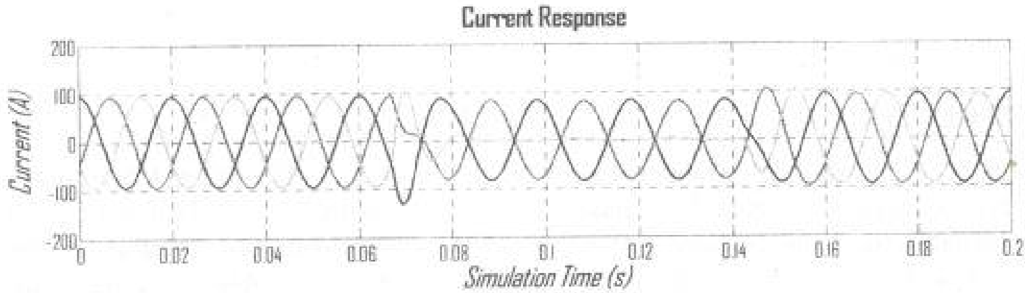

(h) Current Behaviour under a Line-to-Line Fault between the Red and the Yellow Phases.

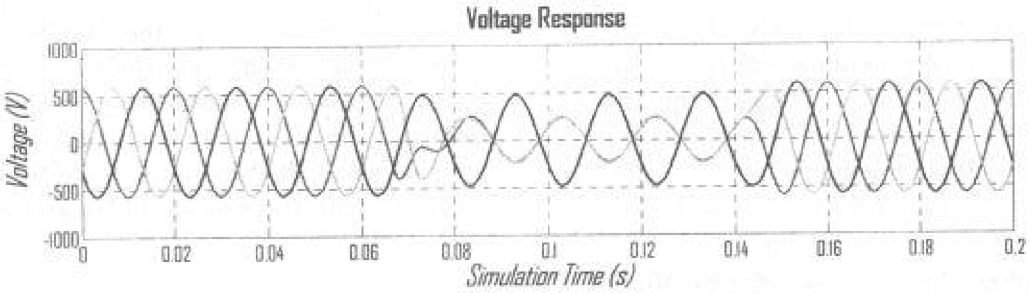

(i) Voltage Behaviour under a Double Line-to-Ground Fault on the Red and the Yellow Phases.

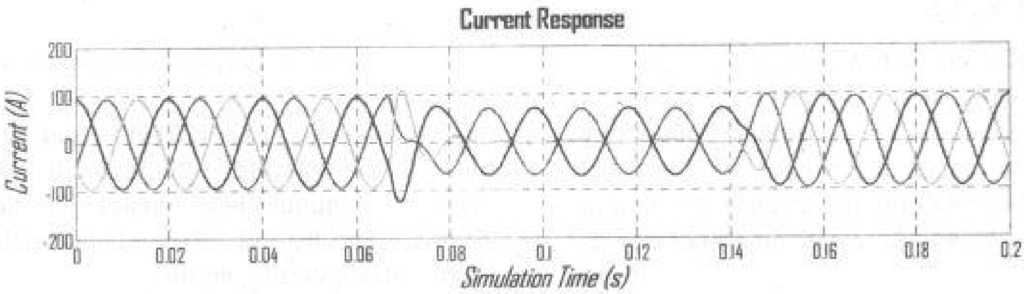

(j) Current Behaviour under a Double Line-to-Ground Fault on the Red and the Yellow Phases.

III. SYSTEM PARAMETERS

Table 1: PV Generator Parameters:

Parameter	Value	Unit
Area of a solar-cell, A	$4x10^{-4}$	m^2
Number of cell string per array, α	32	-
Number of cell per string, β	1000	-
Cell's fill factor, γ	0.864	-
Cell's ideality factor, n	1.93	-
Cell's band-gap energy, E_g	1.42	eV
Conversion efficiency of the cell	24.8	%
Cell's open circuit voltage, V_{oc}	1.03	V
Temperature coefficient, K	0.00015	A/K
Temperature of operation, T_c	315	K
Solar intensity of operation, G	900	W/m^2
DC-Link capacitor, C_{dc}	3500	μF
minimum DC-bus voltage, V'_{dc}	1020	V
VSI switching frequency, f_s	10	KHz
Filter's resistance, R_f	1	mΩ
Filter's inductance, L_f	33.8	mH
Overload factor, a	1.2	-
DC-bus voltage recovery time, t	325	msec
Filter's capacitance, C_f	330	μF
Filter's capacitance, C_f	330	μF
Time constant, τ	1	μs

Table 2: Interface Transformer Parameter:

Parameter	Value	Unit
Nominal power	2.0	MVA
Transformation voltage	0.415/11	kV
Primary impedance, Z_1	0.09+j0.002	Ω
Secondary impedance, Z_2	12.5+j2.07	Ω
Magnetizing impedance, Z_m	6.9+j1.57	Ω

Table 3: Utility Grid Parameter:

Parameter	Value	Unit
Generator's nominal power	100	MVA
Generator's nominal voltage	15	kV
Generator's mechanical power	1.0	p.u
Generator's terminal voltage	0.73	p.u
Generator's internal impedance	0.02+j0.3	p.u
Distribution line length (L_1=L_2)	20	Km
Line resistance	0.7	Ω/km/ph.
Line inductance	0.06632	mH/km/ph.

V. CONCLUSION

The transient behavior and performance of a simulated grid-connected PV generator has been investigated in this paper. Following the application of a three phase symmetrical short-circuit for about 67 milli-seconds, the terminal variables were seen to undergo damped oscillations. At the point of common coupling of the PV generating sub-system and the grid, there was a total collapse of the 11kV voltage with a corresponding current rise from 10A to 150A. While the grid voltage remained undisturbed under the symmetrical short circuit, the grid current shot up from 100A to 250A. A large dip was experienced on the load, as the load voltage fell from 11kV to 10kV while the load current fell from 95A to 75A. The simulation waveforms also revealed the stability problem caused by the application of non-symmetrical short-circuits. The system however regained its initial stable conditions immediately the faults were cleared. The study concluded that by providing necessary paralleling equipments, protective devices and standard means of faults isolation, PV generators could be safely interfaced with the existing utility grid across the country.

REFERENCES

[1] Abou-Khalil, G.A.; Lee, D.C.; Seok, J.K.; Choi J.W. and Kim, H.G. (2007): 'Maximum Power Point Tracking Controller Connecting PV System to Grid', School of Electrical Engineering and Computer Science, Yeungnam University, Korea. Accessed on December 2, 2009 from http://www.yuplc.yuac.kr/paper/internationalI/conference/07.

[2] Ajewole, T.O. (2010): 'Fault Analysis on Grid-Integrated Photovoltaic Power System', Unpublished Master of Science Thesis, Faculty of Technology, Obafemi Awolowo University, Ile-Ife.

[3] Dash, P.P. and Yazdani, A. (2008): 'Mathematical Modeling and Performance Evaluation of a Single-Stage Grid-Connected Photovoltaic (PV) System', *International Journal of Emerging Electric Power*, Volume 9, Issue 6, Article 5, pp 1-32.

[4] Jou H.L.; Chiang, W.J. and Wu, J.C. (2008): 'Simplified Control Method for the Grid-Connected Inverter with the function of Islanding Detection', *IEEE Transaction on Power Electronics*, Volume 23, Number 6, November 2008, pp 2775-2783.

[5] Loh, C.P.; Lai, Y.S.; Chua, G.T. and Li, Y (2005): 'Pulse-Width Modulation of Z-Source Inverters', *IEEE Transactions on Power Electronics*, Volume 20 Number 6, November 2005, pp 1346-1355.

[6] Nikraz, M.; Dehbonei, H. and Nayar, C. (2003): 'A DSP-Controlled Photovoltaic System with Maximum Power Point Tracking', Center for Renewable Energy and Sustainable Technologies, Australia. Accessed on February 3, 2010 from http://www.itee.uq.edu.au/~aupec/aupec03/papers.htm.

[7] Patcharaprakiti N.; Premrudeepreechacharm, S. and Sriuthaisiriwong, H. (2008): 'Maximum Power Point Tracking Using Adaptive Fuzzy Logic Control For Grid-Connected Photovoltaic System', Department of Electrical Engineering, Rajamagala Institute of Technology, Thailand. Accessed on October 11, 2009 from http://www.thaiscience.info/Article.

[8] Ryu, H.M.; Kim, J.H. and Sul, S.K. (2005): 'Analysis of Multiphase Space Vector Pulse-Width Modulation Based on *d-q* Space Concept', *IEEE Transactions on Power Electronics*, Volume 20, Number 6, November 2005, pp 1364-1371.

[9] Singh, B.; Jayaprakash, P and Kothari D.P. (2008): 'A T-Connected Transformer and Three-Leg VSC-Based DSTATCOM for Power Quality Improvement', *IEEE Transactions on Power Electronics*, Volume 23, Number 6, November 2008, pp 1364-1371.

[10] Tsai, H.; Tu, C. and Su, Y. (2008): 'Development of Generalized Photovoltaic Model Using MATLAB/SIMULINK', Proceedings of the World Congress on Engineering and Computer Sciences, October 2008. Accessed on October 11, 2009 from http://www.iaeng.org/publication/WCEC2008.